THE JOURNAL OF PHYSICAL CHEMISTRY B

Article

Cite This: J. Phys. Chem. B 2017, 121, 7681-7688

pubs.acs.org/JPCB

Role of Dispersive Fluorous Interaction in the Solvation Dynamics of the Perfluoro Group Containing Molecules

Saptarsi Mondal,[§,†] Soumit Chatterjee,[§,†] Ritaban Halder,[§,‡] Biman Jana,*[,‡] and Prashant Chandra Singh*[,†]

[†]Department of Spectroscopy, and [‡]Department of Physical Chemistry, Indian Association for the Cultivation of Science, Kolkata, India

Supporting Information

ABSTRACT: Perfluoro group containing molecules possess an important self-aggregation property through the fluorous (F···F) interaction which makes them useful for diverse applications such as medicinal chemistry, separation techniques, polymer technology, and biology. In this article, we have investigated the solvation dynamics of coumarin-153 (C153) and coumarin-6H (C6H) in ethanol (ETH), 2-fluoroethanol (MFE), and 2,2,2-trifluoroethanol (TFE) using the femtosecond upconversion technique and molecular dynamics (MD) simulation to understand the role of fluorous interaction between the solute and solvent molecules in the solvation dynamics of perfluoro group containing molecules. The femtosecond upconversion data show that the time scales of solvation dynamics of C6H in ETH, MFE, and TFE are approximately the same whereas the solvation dynamics of C153 in TFE is slow as compared to that of ETH and MFE. It has also been observed that the time scale of solvation dynamics of C6H in ETH and MFE is higher than that of C153 in the same solvents. MD simulation results show a qualitative agreement with the experimental data in terms of the time scale of the slow components of the solvation for all the systems. The experimental and simulation studies combined lead to the conclusion that the solvation dynamics of C6H in all solvents as well as C153 in ETH and MFE is mostly governed by the charge distribution of ester moieties (C═O and O) of dye molecules whereas the solvation of C153 in TFE is predominantly due to the dispersive fluorous interaction (F···F) between the perfluoro groups of the C153 and solvent molecules.

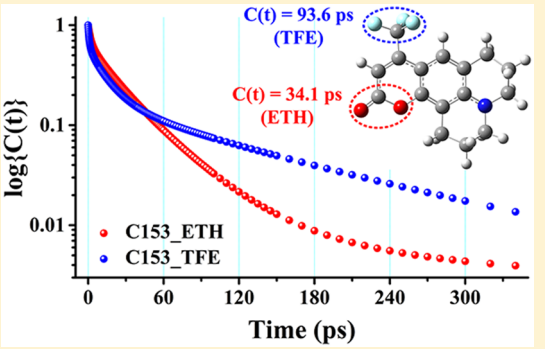

INTRODUCTION

Extensive research efforts have been devoted to design the noncanonical amino acids, especially the fluorocarbon-substituted amino acids, to incorporate the recombinant proteins in order to modulate the physicochemical properties of proteins in a controlled manner.[1−7] In fact, several experimental and molecular dynamics (MD) simulation studies have shown that the fluorination of the helix bundle and coiled proteins increases its stability against the chemical and thermal denaturation without affecting much in their structure as well as biological activity.[6,8−10] Apart from the biology, fluorinated molecules have been used extensively in other fields such as medicinal chemistry, polymer industry, and separation techniques.[11−16] It has been shown that the fluoro-substituted polymers are nonsticky as well as friction-reducing, and as a result they have been extensively used for the coating of optical fibers, thermoplastics, and elastomers.[12] It has been also found that the selectivity as well as quantum yield of several organic reactions have been enhanced when they were performed in the fluorinated mediums.[13,14]

Substitution of fluorocarbon (C−F) in place of hydrocarbon (C−H) provides unique but important physicochemical properties to molecules. Both fluorocarbons and hydrocarbons are hydrophobic in nature, but they differ in other ways.[15,17] The C−F group is highly polar and less polarizable due to the high electronegativity as well as small size of fluorine. The dipole moment of C−F is higher than that of the C−H bond, and the direction of the dipole of the C−F is opposite to that of the C−H. The higher dipole moment of C−F generates strong inductive effect, which creates strong electrostatic interaction with the polar groups. Indeed, due to this induced polar nature, the hydrophobicity of C−F has been described as polar hydrophobicity.[18] Moreover, the C−F bond is longer than the C−H bond which increases the volume of C−F containing molecules as compared to the C−H ones. These unique properties of the C−F group endues them with self-aggregation properties through weak fluorous (F···F) interactions.

Due to the unique nature of the C−F group, several groups have attempted to understand the photophysical as well as hydration phenomena of molecules containing the C−F group. Krishnamoorthy and co-workers have shown that the replacement of tryptophan by 5-fluorotryptophan decreases

Received: April 11, 2017
Revised: July 19, 2017
Published: July 24, 2017

DOI: 10.1021/acs.jpcb.7b03420
J. Phys. Chem. B 2017, 121, 7681−7688

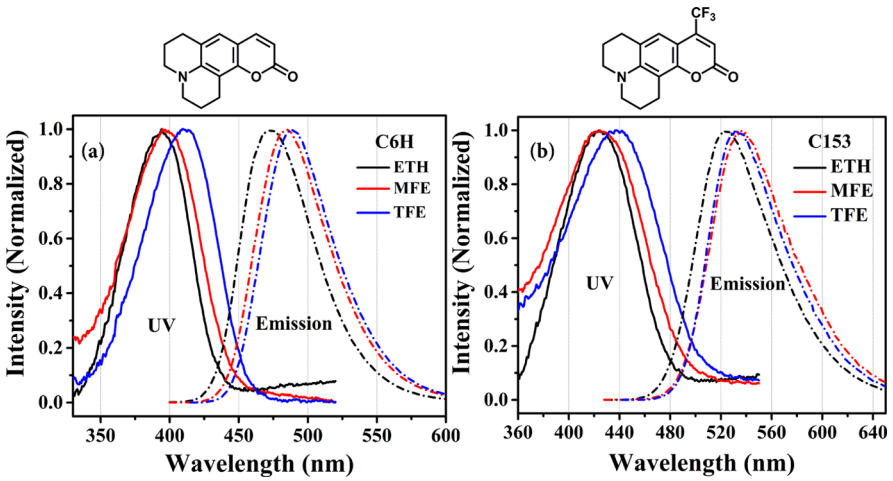

Figure 1. Structures of C6H (left) and C153 (right) along with their absorption and emission spectra in ETH (black), MFE (red), and TFE (blue), respectively. The absorption spectra are shown as solid lines whereas the emission spectra are shown as broken lines.

the heterogeneity of proteins.[19] Knutson and co-workers have shown that 5F-tryptophan slows down and suppresses electron transfer quenching as well as significantly masking pseudo-time-dependent fluorescence Stokes' shift in monellin protein and thereby helps to provide a clear observation on the ultrafast relaxation explicitly due to solvent and protein response.[20] Zewail and co-workers have studied the effect of surface fluorination on the water−protein dynamics and found that the fluorinated side chains exert strong electrostatic drag on the neighboring water molecules which slows down the water motion more at the fluorinated surface as compared to the nonfluorinated ones.[21] Recently, we have studied the behavior of probe molecules containing the perfluoro group ($-CF_3$) in the presence and absence of solvents having the perfluoro group to understand the role of fluorous interaction between the solute and solvents molecules on their photophysical properties.[22] We have shown that the perfluoro group of TFE has a preferential organization around the $-CF_3$ group of coumarin 153 (C153). Molecular dynamics snapshots as well as radial distribution function analysis were presented in (ref 22) to manifest solvent organization around coumarin dyes in different fluorinated alcohols. The radial distribution function analysis indicates a preferential solvation through the $-CF_3$ end of 2,2,2-trifluoroethanol (TFE) rather than its oxygen end of OH group around perfluoro group of C153. We have also shown that in 2-fluoroethanol (MFE), the $-CF_3$ group of C153 prefers to have a $CF_2-F\cdots H-(CHF)$ kind of electrostatic interaction over the $CF_2-F\cdots F-(CH_2)$ type of dispersion interaction. On the other hand, in TFE, the $-CF_3$ group of coumarin 153 prefers to have a C−F···F−C type dispersion interaction. Hence, the next question arises as to whether the fluorous interaction plays any significant role in the solvation process as well, if the probe and solvents both contain the perfluoro groups.

In order to get the answer to the above question, we have applied femtosecond upconversion as well as MD simulation techniques to study the solvation behavior of two prototypical dyes coumarin-6H (C6H) and C153 (structures are depicted in Figure 1) in ethanol (ETH), MFE, and TFE solvents. Both dyes have the same skeleton except for the presence of perfluoro group in C153. We have used two different fluorinated-ETHs along with ETH to have a systematic understanding of the solvation process of these two dyes in fluorinated solvents. The femtosecond upconversion and MD simulation data clearly reveal that the solvation dynamics of C6H in all the solvents and C153 in ETH and MFE is mostly governed by the charge distribution of ester moieties (C═O and O) of the dye molecules whereas the solvation of C153 in TFE is predominantly due to the dispersive fluorous interaction (F···F) between the perfluoro groups of the C153 and TFE molecules.

METHODS

Absorption spectra were measured using a UV−vis spectrophotometer (Thermo Fisher Scientific Evolution 201). The O.D. was kept below 0.1 for steady state experiments in order to avoid inner filter effect. Steady state fluorescence emission spectra were recorded with a fluoromax 4 (HORIBA Scientific) spectrofluorometer. In order to investigate the early time dynamics, i.e., in the picosecond−femtosecond regime, femtosecond optical gating technique was used. The detailed description of the upconversion setup used in this study has been mentioned elsewhere.[23] Briefly, the sample was excited at 390 and 420 nm for C6H and C153, respectively, using the second harmonic of a mode-locked Ti:sapphire laser (Tsunami, Spectra Physics) pumped by a 5 W Millennia (Spectra Physics) laser. The fundamental beam, 780 nm (for C6H) or 840 nm (for C153), respectively, was frequency doubled in a nonlinear crystal (1 mm BBO, $\theta = 25°$, $\phi = 90°$) to produce the desired excitation wavelength. The fluorescence signal from the sample was upconverted in a nonlinear crystal (0.5 mm BBO, $\theta = 38°$, $\phi = 90°$) using the fundamental beam as a gate pulse. The upconverted light was dispersed into a monochromator and detected using photon counting electronics. The fluorescence decays were recorded at the magic angle polarization with respect to the excitation pulse. The full width at half-maximum (fwhm) of the cross-correlation function of the upconversion instrument was found to be ∼280 fs from the Raman scattering of ethanol. The power of the second harmonic signal was intentionally kept low (∼5 mW) using a neutral density filter to avoid the photobleaching of the sample. The femtosecond fluorescence decay profiles were fitted using a Gaussian function of the same "fwhm" as the excitation pulse and by iterative deconvolution using a local program[24] keeping the nanosecond lifetime, found from the TCSPC experiment, fixed at each time. The O.D. of the sample was kept at ∼1.0 for the

DOI: 10.1021/acs.jpcb.7b03420
J. Phys. Chem. B 2017, 121, 7681−7688

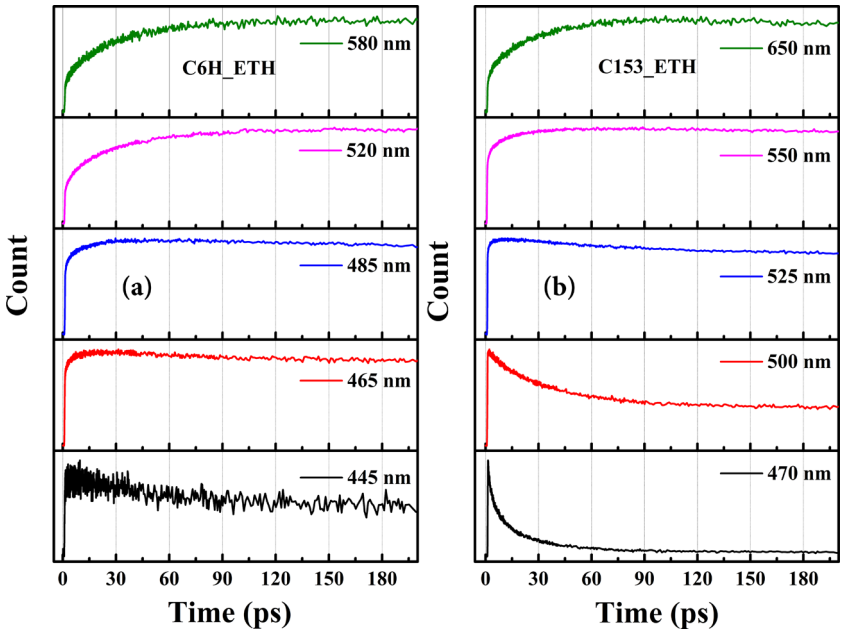

Figure 2. Femtosecond lifetime decay profiles of C6H (a) and C153 (b) in ETH from the blue to red region of the emission spectra.

upconversion measurement as the path length used in the setup was 1 mm. Absorption and emission spectra were measured before and after upconversion measurements to ensure the stability of the sample against photobleaching and the reliability of data. The time-resolved emission spectra (TRES) were constructed using the best fit parameters of the femtosecond fluorescence decays and steady state emission intensities proposed by Maroncelli and Fleming.[25−29] The relaxation of solvent around the newly formed excited state dipole of the probe created by femtosecond pulses leads to the red-shift of the fluorescence spectrum. This shift in the TRES spectrum can be represented as $C(t)$ according to the following equation

$$C(t) = \frac{\{\nu(t) - \nu(\infty)\}}{\{\nu(0) - \nu(\infty)\}}$$

where $\nu(0)$, $\nu(t)$, and $\nu(\infty)$ are emission peak frequencies at 0, t, and ∞ time, respectively; generally $\nu(\infty)$ is the peak frequency found from the steady state fluorescence spectrum. $C(t)$ may also be written as

$$C(t) = \frac{\{E(t) - E(\infty)\}}{\{E(0) - E(\infty)\}}$$

where $E(0)$, $E(t)$, and $E(\infty)$ are the solvation energy of solute at 0, t, and ∞ time, respectively. When the perturbation is small, according to the linear response theory, the experimentally measured nonequilibrium solvation time correlation function can be equated to the equilibrium fluctuation autocorrelation function of the total energy of the dye which is commonly referred as equilibrium solvation time correlation function $C_S(t)$[30]

$$C_S(t) = \frac{\langle \Delta E(0) \Delta E(t) \rangle}{\langle \Delta E(0) \Delta E(0) \rangle}$$

where $\Delta E(t) = E(t) - \overline{E(t)}$ is the time-dependent fluctuation of the total energy of dye molecule, $E(t)$, and $\overline{E(t)}$ is the total energy and the average energy of dye molecule at time t, respectively. Next, $C_S(t)$ is fitted with a triexponential formula as $C_S(t) = a_0 \exp(-t/a_1) + a_2 \exp(-t/a_3) + (1 - a_0 - a_2) \exp(-t/a_4)$, where α_1, α_3, and α_4 are the characteristic time constants. We have performed MD simulations of C153 and C6H in ETH, MFE, and TFE using the GROMACS (GROMACS version 4.6.5) package.[31] The automated topology builder (ATB) software[32] has been utilized to generate the parameters of both C153 and C6H. In the case of ETH and TFE, we have considered the united atom parameters of GROMOS53a6 force field.[33] The perfluoro group was described by four explicit atoms (one carbon and three fluorine atoms), and methylene (and methyl) group was described as a single carbon atom. The topology of MFE was constructed by attaining its correct density. All the simulations have been started with the structures of C153 and C6H which were optimized by ATB, and then solvation of these dyes has been done in different solvents. For dye molecules, the similar atom descriptions were used as solvents. The partial charges on each atom of the dye molecules are listed in Figure S3 of the Supporting Information. The steepest descent energy minimization has been performed to all systems. The solvated system was equilibrated in NPT condition for 10 ns at 300 K temperature and 1 bar pressure for all cases. The NPT production run to all the equilibrated system was performed using a Nose−Hoover[34] thermostat (with a time constant value of 0.5 ps^{-1}) and Parrinello−Rahmann barostat[35] (with a time constant value of 1.0 ps^{-1}) to maintain the temperature and pressure. For each of the simulations, we have used a time step of 1 fs with periodic boundary conditions. Electrostatic interactions were handled by particle Mesh Ewald (PME) calculation.[36] with a grid pacing of 0.16 nm and an interpolation order of 4. The neighbor list was generated at every 10 steps. The trajectories were saved at every 20 fs interval for the calculation of relevant quantities. In this study, we have used 1970 solvent molecules along with 1 dye molecule in a cubic box of 7.0 nm. A cutoff radius of 1.0 nm has been used for both neighbor list search and van der Waals interaction. The 20 ns simulation for each of the dye−solvent systems has been performed.

DOI: 10.1021/acs.jpcb.7b03420
J. Phys. Chem. B 2017, 121, 7681−7688

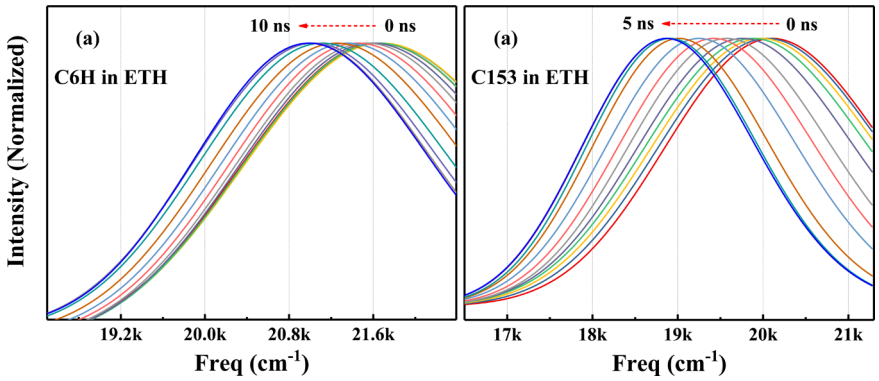

Figure 3. Time-resolved emission spectra (TRES) of C6H (a) and C153 (b) in ETH.

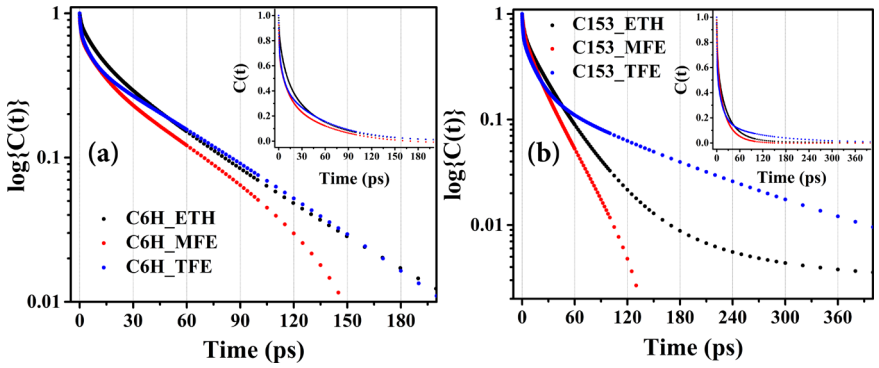

Figure 4. Plots of solvent relaxation time ($C(t)$) (in log scale) of C6H (a) and C153 (b) in ETH (black), MFE (red), and TFE (blue). The linear scale plots of $C(t)$ of C6H and C153 in the respective solvents are provided in the insets.

Table 1. Amplitude and Time Components of the $C(t)$ of C153 and C6H in ETH, MFE, and TFE Obtained from the Fluorescence Upconversion Study[a]

system	τ_1	a_1	τ_2	a_2	τ_3	a_3	τ_{av}
				C6H			
ETH	0.70 ± 0.04	0.14 ± 0.03	8.88 ± 0.09	0.35 ± 0.04	48.92 ± 1.61	0.51 ± 0.02	28.19 ± 0.02
MFE	0.61 ± 0.07	0.28 ± 0.02	8.88 ± 0.28	0.31 ± 0.02	55.75 ± 0.66	0.41 ± 0.00	25.70 ± 0.11
TFE	0.46 ± 0.01	0.23 ± 0.02	5.47 ± 0.63	0.31 ± 0.03	55.77 ± 3.86	0.46 ± 0.03	27.38 ± 0.14
				C153			
ETH	1.62 ± 0.13	0.29 ± 0.01	10.13 ± 0.42	0.21 ± 0.02	34.08 ± 0.45	0.50 ± 0.01	19.36 ± 0.01
MFE	1.57 ± 0.08	0.28 ± 0.03	9.39 ± 0.18	0.27 ± 0.03	28.40 ± 0.62	0.45 ± 0.03	15.66 ± 2.32
TFE	0.85 ± 0.04	0.38 ± 0.02	12.17 ± 0.15	0.42 ± 0.01	93.61 ± 0.48	0.19 ± 0.03	23.18 ± 2.10

[a]The time components are in units of picosecond.

RESULTS AND DISCUSSION

Figure 1 shows the structures of C6H and C153 as well as the steady state absorption and emission spectra of C6H and C153 in ETH, MFE, and TFE, respectively. The peak position of the absorption and emission spectra of C6H and C153 get red-shifted in fluorinated-ETHs as compared to ETH. However, there is a noticeable difference in the emission spectra of C153 in fluorinated-ETHs as compared to C6H. The emission spectrum of C153 in TFE is blue-shifted as compared to MFE whereas the emission spectrum of C6H in TFE is more red-shifted than MFE which indicates that the local surrounding of C153 in TFE is different from that of C6H.

In order to realize the solvation behavior of these two dyes in ETH, MFE, and TFE, we have calculated the solvent correlation time $C(t)$ by measuring the TRES using the femtosecond upconversion technique. Around 25 fluorescent decay curves have been measured for each sample from the blue to red edge of the respective emission spectrum. Figure 2 shows the typical time traces of C6H and C153 in ETH from the blue region to the red region of the steady state emission spectra. The time trace profiles show ultrafast decay component along with long time decay component at the blue edge of the emission spectra, whereas it shows an ultrafast rise component along with a long time decay component in the red region of emission spectra. A similar nature of time traces has been found for the C6H as well as C153 in MFE and TFE as shown in Figure S1. The observed decay behavior of time traces at the blue region and the rise at the red region of the emission spectrum are the characteristic features of the solvation process, and such features have been shown earlier for many different systems.[26,37−46] Time traces have been fitted with the sum of exponentials. Further, we have constructed the TRES for these two dyes in ETH, MFE, and TFE using their respective best fitting parameters obtained from their decay time traces. Figure 3 shows the TRES of C6H and C153 in ETH, whereas the

DOI: 10.1021/acs.jpcb.7b03420
J. Phys. Chem. B 2017, 121, 7681−7688

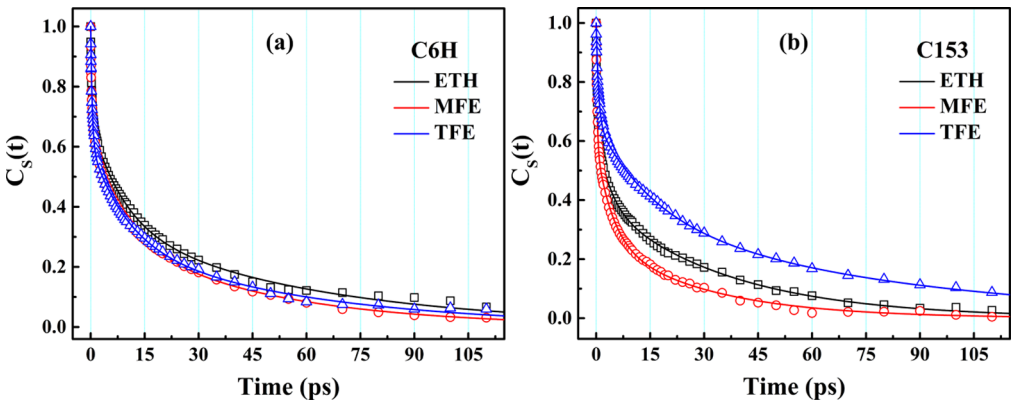

Figure 5. $C_s(t)$ of C6H (a) and C153 (b) in ETH (black), MFE (red), and TFE (blue). The solid lines represent the best fit of the plots.

TRES profiles for C6H and C153 in MFE and TFE are provided in the Supporting Information (Figure S2). Log-normal fits to TRES are used for calculating the time-dependent Stokes shifts in terms of first moment (mean) frequency shifts.

Figure 4 shows the $C(t)$ of C6H and C153 in ETH, MFE, and TFE solutions, respectively. The $C(t)$ for both dyes in ETH, MFE, and TFE were fitted with three exponentials, and the values of their amplitudes, solvation time components, as well as average solvation time are provided in Table 1. The three components of $C(t)$ for C153 in ETH were found to be 1.6, 10.1, and 34.1 ps, respectively, yielding the average solvation time to be 19.4 ps, which is in good agreement with the earlier reports of Maroncelli and co-workers.[25,28] Fast components (1.6 and 10.1 ps) of $C(t)$ have been assigned to the inertial nature of solvation, whereas the slow component (~30 ps) of $C(t)$ has been assigned to the diffusive nature of solvation by Maroncelli and co-workers based on their extensive theoretical and experimental studies on the solvation of C153 in different types of solvents.[27,29,43,47,48] The inertial nature of solvation has been assigned mainly to the libration mode as well as hindered libration mode of solvent molecules, whereas diffusive nature of solvation has been attributed mainly to the viscosity of the solvent medium as well as specific solute−solvent interaction.[48−50]

It can be observed that the average $C(t)$ for C6H in ETH, MFE, and TFE is approximately the same within the experimental uncertainty. However, the average $C(t)$ of C153 in TFE is higher as compared to ETH and MFE. Noticeably, the first two components of the $C(t)$ for both dyes in all solvents are approximately same within the experimental uncertainty. However, the third component of $C(t)$ of C153 in TFE (93.6 ps) is ~3 times larger as compared to ETH (34.1 ps) and MFE (28.4 ps), whereas it is approximately the same for C6H in all the solvents. The trend of $C(t)$ values clearly indicates that the solvation of C153 in TFE is different from that of C6H. Interestingly, unlike C153 in TFE, the average $C(t)$ as well as the last component of $C(t)$ of C6H in ETH and MFE is higher than C153 which suggests that the specific interaction between C153 and TFE can be an important player in their slow solvation time scale.

To investigate the molecular origin of slower solvation time scale of C153 in TFE, we have performed equilibrium molecular dynamics simulation of C153 and C6H in ETH, MFE, and TFE. The experimentally measured nonequilibrium $C(t)$ can be equated to the equilibrium fluctuation autocorrelation function of the total energy of the dye which is commonly referred as equilibrium solvation time correlation function, $C_s(t)$. Hence, we have calculated the $C_s(t)$ of C153 and C6H dye in ETH, MFE, and TFE using MD simulations. The results obtained from our calculations have been presented below in Figure 5 where the plots of $C_s(t)$ are fitted with triexponential decay and the obtained values of parameters have been shown in Table 2. The time components of $C_s(t)$ of C153 in different solvents clearly show that $C_s(t)$ values of C153 in TFE have a significantly slower component (77 ps) than ETH (35 ps) and MFE (29 ps). The components of $C_s(t)$ of C6H in ETH, MFE, and TFE are approximately the same within the uncertainty of the calculations. The time scales of the slow component of $C_s(t)$ of C6H in ETH and MFE are higher than that of C153 in the same solvents. The simulation results do not match quantitatively with the experimental values; nevertheless, they are in qualitatively good agreement.

Table 2. Calculated Amplitude and Time Components of the $C_s(t)$ of C153 and C6H in ETH, MFE, and TFE Obtained from the MD Simulation[a]

	τ_1	a_1	τ_2	a_2	τ_3	a_3
			C6H			
ETH	0.30	0.31	8.98	0.33	50.0	0.36
MFE	0.09	0.30	1.95	0.25	44.0	0.45
TFE	0.30	0.32	8.27	0.35	48.0	0.33
			C153			
ETH	0.24	0.36	3.63	0.23	35.7	0.41
MFE	0.26	0.41	4.47	0.31	29.9	0.28
TFE	0.65	0.33	15.14	0.29	77.0	0.38
			C6H (charge modified)			
ETH	0.22	0.30	3.86	0.22	33.6	0.48
TFE	0.23	0.37	5.54	0.34	38.6	0.37
			C153 (only CF_3 part)			
TFE	0.17	0.64	5.45	0.25	68.1	0.11
TFE(Cou)	0.35	0.61	4.86	0.31	40.1	0.08
TFE(LJ)	0.15	0.68	4.18	0.21	62.2	0.11

[a]The time components are in units of picosecond. C6H (charge modified) represents the condition when the charges of the C═O and O of C6H have been replaced with C153. C153 (only CF_3 part) means the $C_s(t)$ of C153 has been calculated explicitly by considering only the energy of the $-CF_3$ group of the molecule. Cou and LJ stand for the Coulombic and Lennard-Jones energies, respectively.

First, we have focused on understanding the slower solvation dynamics of C6H as compared to C153 in ETH and MFE. In order to realize the origin of slower $C(t)$ of C6H in ETH, we

DOI: 10.1021/acs.jpcb.7b03420
J. Phys. Chem. B 2017, 121, 7681−7688

have calculated the $C_s(t)$ of C6H in ETH and TFE by changing the partial charges on both the oxygen atoms of C6H (C═O and O) with the partial charges of oxygen atoms of C153 and tuning other charges minimally to preserve the neutrality of the molecule. Swapping of charges on the oxygen atoms have been done to exclude the effect of the CF_3 group of the C153 and making the molecule environment of C6H similar to that of C153. The calculated $C_s(t)$ values of modified C6H in ETH and TFE are shown in Figure 6, and values of the parameters

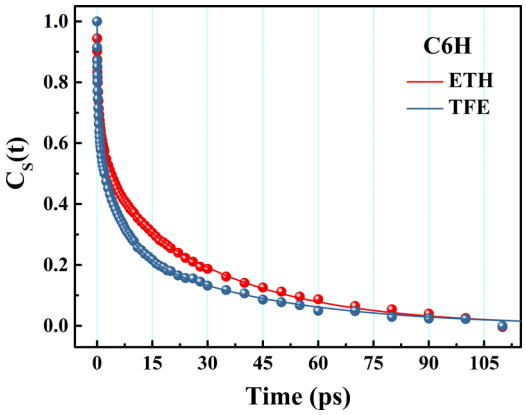

Figure 6. $C_s(t)$ calculation of C6H in ETH (red) and TFE (cyan) on replacing the charges on C═O and O of C6H with C153.The solid lines represent the best fit of the plots.

are provided in Table 2. It can be seen that the slow component of modified $C_s(t)$ of C6H in ETH is ∼33.6 ps, which is very close to the $C_s(t)$ of C153 (35.6 ps) in the same solvent clearly stating that higher charge on the oxygen sites of the C6H causes the higher $C(t)$ of C6H than that of C153 in ETH. Moreover, the $C_s(t)$ of modified C6H in TFE is ∼38.6 ps which is less than the $C_s(t)$ of C153 (77.0 ps) in the same solvent indicating that the $-CF_3$ group of the C153 plays a significant role in the slow component of the solvation in TFE.

Finally, to uncover the molecular basis of the slow time component of C153 in TFE, the structural difference between C153 and C6H has been considered. The structural motif of C6H and C153 is almost the same except for the presence of the CF_3 group on C153. Our earlier study regarding the solvent organization around C153 indicates that the CF_3 group of TFE has a preferential arrangement around the perfluoro group of C153 which is the reason behind the different photophysical behavior of C153 in TFE as compared to other fluorinated-ETHs.[22] To investigate the role of perfluoro group of C153 in the slow component of $C(t)$ of C153 in TFE, we have calculated equilibrium $C_s(t)$ by considering explicitly the energy of the $-CF_3$ group of C153 in TFE, and the result is shown in Figure 7a and Table 2. The components of $C_s(t)$ of C153 in TFE again show the slow component (68 ps) which is very close to the slow component of $C_s(t)$ (77 ps) when the energy of whole molecule is considered. This indicates that the $-CF_3$ group has direct influence on the emergence of the slow component of $C_s(t)$ of C153 in TFE. In order to get more comprehensive understanding behind the role of $-CF_3$ group in the slow component of $C_s(t)$ of C153 in TFE, we have decomposed $C_s(t)$ further into Coulombic and Lennard-Jones part. The decay profiles of the decomposed parts of $C_s(t)$ are shown in Figures 7b and c, and the values of the fitting parameters for these decays are provided in Table 2. The slow component of $C_s(t)$ for the Lennard-Jones part (dispersive interaction) is ∼63 ps whereas it appears to be ∼40 ps for the Coulombic part. The slow component of $C_s(t)$ of C153 in TFE for the Lennard-Jones part is closer to the without decomposed $C_s(t)$ value (77 ps) as well as observed experimental $C(t)$ value (93 ps) indicating that the slow component of the C153 in TFE is mainly originating from the dispersive interaction between the CF_3 groups of C153 and TFE, and the contribution of the Coulombic part is not significant. This study clearly describes that the solvation dynamics of C6H in all the solvents as well as C153 in ETH and MFE are mostly determined by the charge distribution of ester moieties (C═O and O) of the dye molecules. However, solvation dynamics of C153 in TFE is primarily governed by the perfluoro ($-CF_3$) group of the dye molecule which creates dispersive fluorous interaction (F···F) between the $-CF_3$ group of the dye and TFE molecules.

CONCLUSION

We have investigated the solvation dynamics of C153 and C6H in ETH, MFE, and TFE using the femtosecond upconversion and MD simulation methods in order to understand the role of fluorous interaction in the solvation dynamics of the perfluoro group containing molecules. The results obtained from the femtosecond upconversion studies show that time scales of the solvation dynamics of C6H in ETH, MFE, and TFE are approximately the same whereas the solvation dynamics of C153 in TFE is slow as compared to those in ETH and MFE. It has also been observed that the solvation dynamics of C153 in ETH and MFE is less than that of C6H in the same solvents. MD simulation results show a qualitative agreement with the

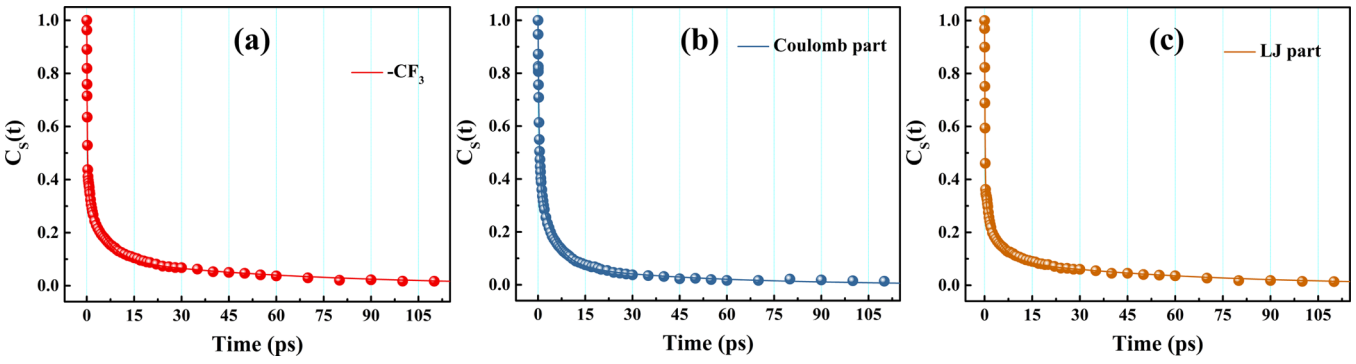

Figure 7. (a) $C_s(t)$ calculation of C153 in TFE on explicit consideration of the energy of $-CF_3$ group of molecules. (b) and (c) describe the Columbic and Lennard-Jones part of the $C_s(t)$ of C153 in TFE on explicit consideration of the energy of the $-CF_3$ group of molecules.

DOI: 10.1021/acs.jpcb.7b03420
J. Phys. Chem. B 2017, 121, 7681−7688

experimental results in terms of the time scales of the slow components of the solvation in all the systems. Based on experimental and simulation results, it has been concluded that the solvation dynamics of C6H in all the solvents and C153in ETH and MFE is mostly governed by the charge distribution of ester moieties (C═O and O) of the dye molecules whereas the slow component of the C153 in TFE is predominantly due to the dispersive fluorous interaction (F···F) between the perfluoro groups of the C153 and TFE molecules. Our study demonstrates that the fluorous interaction is a key player in the solvation dynamics of the perfluoro group containing molecules.

■ ASSOCIATED CONTENT

Supporting Information

The Supporting Information is available free of charge on the ACS Publications website at DOI: 10.1021/acs.jpcb.7b03420.

Time-resolved traces as well as time-resolved emission plots of C6H and C153 in MFE and TFE solvents; charge distributions of C6H and C153 (PDF)

■ AUTHOR INFORMATION

Corresponding Authors

*E-mail: sppcs@iacs.res.in.

*E-mail: pcbj@iacs.res.in.

ORCID

Biman Jana: 0000-0001-7684-1963

Prashant Chandra Singh: 0000-0001-9357-9039

Author Contributions

§These authors contributed equally to this work.

Notes

The authors declare no competing financial interest.

■ ACKNOWLEDGMENTS

This work is supported partially by the research grants provided by the Council of Scientific and Industrial Research (CSIR) [Grant No. 01(2803)/14/EMR-II] as well as Department of Science and Technology (DST-SERB) [Grant No. EMR/2015/001605] India. S.M, S.C., and R.H. thank Institute, DST, and CSIR for their fellowships, respectively. We also acknowledge our sincere thanks to Prof. Anindya Dutta for the use of his upconversion setup for the time-resolved measurements.

■ REFERENCES

(1) Buer, B. C.; Marsh, E. N. G. Fluorine: A New Element in Protein Design. *Protein Sci.* **2012**, *21*, 453−462.

(2) Buer, B. C.; Levin, B. J.; Marsh, E. N. G. Influence of Fluorination on the Thermodynamics of Protein Folding. *J. Am. Chem. Soc.* **2012**, *134*, 13027−13034.

(3) Yoo, T. H.; Link, A. J.; Tirrell, D. A. Evolution of a Fluorinated Green Fluorescent Protein. *Proc. Natl. Acad. Sci. U. S. A.* **2007**, *104*, 13887−13890.

(4) Jäckel, C.; Salwiczek, M.; Koksch, B. Fluorine in a Native Protein Environment—How the Spatial Demand and Polarity of Fluoroalkyl Groups Affect Protein Folding. *Angew. Chem., Int. Ed.* **2006**, *45*, 4198−4203.

(5) Lee, K.-H.; Lee, H.-Y.; Slutsky, M. M.; Anderson, J. T.; Marsh, E. N. G. Fluorous Effect in Proteins: De Novo Design and Characterization of a Four-α-Helix Bundle Protein Containing Hexafluoroleucine. *Biochemistry* **2004**, *43*, 16277−16284.

(6) Bilgiçer, B.; Fichera, A.; Kumar, K. A Coiled Coil with a Fluorous Core. *J. Am. Chem. Soc.* **2001**, *123*, 4393−4399.

(7) Neil, E.; Marsh, G. Towards the Nonstick Egg: Designing Fluorous Proteins. *Chem. Biol.* **2000**, *7*, R153−R157.

(8) Montclare, J. K.; Son, S.; Clark, G. A.; Kumar, K.; Tirrell, D. A. Biosynthesis and Stability of Coiled-Coil Peptides Containing (2S,4R)-5,5,5-trifluoroleucine and (2S,4S)-5,5,5-trifluoroleucine. *ChemBioChem* **2009**, *10*, 84−86.

(9) Tang, Y.; Tirrell, D. A. Biosynthesis of a Highly Stable Coiled-Coil Protein Containing Hexafluoroleucine in an Engineered Bacterial Host. *J. Am. Chem. Soc.* **2001**, *123*, 11089−11090.

(10) Tang, Y.; Ghirlanda, G.; Petka, W. A.; Nakajima, T.; DeGrado, W. F.; Tirrell, D. A. Fluorinated Coiled-Coil Proteins Prepared In Vivo Display Enhanced Thermal and Chemical Stability. *Angew. Chem., Int. Ed.* **2001**, *40*, 1494−1496.

(11) Biswas, B.; Mondal, S.; Singh, P. C. Combined Molecular Dynamics, Atoms in Molecules, and IR Studies of the Bulk Monofluoroethanol and Bulk Ethanol To Understand the Role of Organic Fluorine in the Hydrogen Bond Network. *J. Phys. Chem. A* **2017**, *121*, 1250−1260.

(12) Narita, T. Synthesis of Novel Fluorinated Polymers: Facile Carbon-Carbon Bond Formation Aided by Fluorine Substituents. *Polym. J.* **2011**, *43*, 497−515.

(13) Clot, E.; Eisenstein, O.; Jasim, N.; Macgregor, S. A.; McGrady, J. E.; Perutz, R. N. C−F and C−H Bond Activation of Fluorobenzenes and Fluoropyridines at Transition Metal Centers: How Fluorine Tips the Scales. *Acc. Chem. Res.* **2011**, *44*, 333−348.

(14) Evans, M. E.; Burke, C. L.; Yaibuathes, S.; Clot, E.; Eisenstein, O.; Jones, W. D. Energetics of C−H Bond Activation of Fluorinated Aromatic Hydrocarbons Using a [Tp′Rh(CNneopentyl)] Complex. *J. Am. Chem. Soc.* **2009**, *131*, 13464−13473.

(15) Müller, K.; Faeh, C.; Diederich, F. Fluorine in Pharmaceuticals: Looking Beyond Intuition. *Science* **2007**, *317*, 1881−1886.

(16) Böhm, H.-J.; Banner, D.; Bendels, S.; Kansy, M.; Kuhn, B.; Müller, K.; Obst-Sander, U.; Stahl, M. Fluorine in Medicinal Chemistry. *ChemBioChem* **2004**, *5*, 637−643.

(17) Dunitz, J. D. Organic Fluorine: Odd Man Out. *ChemBioChem* **2004**, *5*, 614−621.

(18) Biffinger, J. C.; Kim, H. W.; DiMagno, S. G. The Polar Hydrophobicity of Fluorinated Compounds. *ChemBioChem* **2004**, *5*, 622−627.

(19) Sarkar, S. S.; Udgaonkar, J. B.; Krishnamoorthy, G. Reduced Fluorescence Lifetime Heterogeneity of 5-Fluorotryptophan in Comparison to Tryptophan in Proteins: Implication for Resonance Energy Transfer Experiments. *J. Phys. Chem. B* **2011**, *115*, 7479−7486.

(20) Xu, J.; Chen, B.; Callis, P.; Muiño, P. L.; Rozeboom, H.; Broos, J.; Toptygin, D.; Brand, L.; Knutson, J. R. Picosecond Fluorescence Dynamics of Tryptophan and 5-Fluorotryptophan in Monellin: Slow Water−Protein Relaxation Unmasked. *J. Phys. Chem. B* **2015**, *119*, 4230−4239.

(21) Kwon, O.-H.; Yoo, T. H.; Othon, C. M.; Van Deventer, J. A.; Tirrell, D. A.; Zewail, A. H. Hydration Dynamics at Fluorinated Protein Surfaces. *Proc. Natl. Acad. Sci. U. S. A.* **2010**, *107*, 17101−17106.

(22) Mondal, S.; Halder, R.; Biswas, B.; Jana, B.; Singh, P. C. Solvent Organization Around the Perfluoro Group of Coumarin 153 Governs its Photophysical Properties: An Experimental and Simulation Study of Coumarin Dyes in Ethanol as well as Fluorinated Ethanol Solvents. *J. Chem. Phys.* **2016**, *144*, 184504.

(23) Chatterjee, S.; Burai, T. N.; Karuso, P.; Datta, A. Ultrafast Dynamics of Epicocconone, a Second Generation Fluorescent Protein Stain. *J. Phys. Chem. A* **2011**, *115*, 10154−10158.

(24) Chatterjee, S.; Karuso, P.; Boulangé, A.; Franck, X.; Datta, A. Excited State Dynamics of Brightly Fluorescent Second Generation Epicocconone Analogues. *J. Phys. Chem. B* **2015**, *119*, 6295−6303.

(25) Horng, M. L.; Gardecki, J. A.; Papazyan, A.; Maroncelli, M. Subpicosecond Measurements of Polar Solvation Dynamics: Coumarin 153 Revisited. *J. Phys. Chem.* **1995**, *99*, 17311−17337.

(26) Jimenez, R.; Fleming, G. R.; Kumar, P. V.; Maroncelli, M. Femtosecond Solvation Dynamics of Water. *Nature* **1994**, *369*, 471−473.

(27) Fee, R. S.; Maroncelli, M. Estimating the Time-Zero Spectrum in Time-Resolved Emmsion Measurements of Solvation Dynamics. *Chem. Phys.* **1994**, *183*, 235−247.
(28) Maroncelli, M.; Fleming, G. R. Picosecond Solvation Dynamics of Coumarin 153: The Importance of Molecular Aspects of Solvation. *J. Chem. Phys.* **1987**, *86*, 6221−6239.
(29) Castner, E. W.; Maroncelli, M.; Fleming, G. R. Subpicosecond Resolution Studies of Solvation Dynamics in Polar Aprotic and Alcohol Solvents. *J. Chem. Phys.* **1987**, *86*, 1090−1097.
(30) Bagchi, B.; Jana, B. Solvation Dynamics in Dipolar Liquids. *Chem. Soc. Rev.* **2010**, *39*, 1936−1954.
(31) Abraham, M. J.; van der Spoel, D.; Lindahl, E.; Hess, B.; et al.; Gromacs User Manual 5.1.4, www.gromacs.org, 2016.
(32) Canzar, S.; El-Kebir, M.; Pool, R.; Elbassioni, K.; Malde, A. K.; Mark, A. E.; Geerke, D. P.; Stougie, L.; Klau, G. W. Charge Group Partitioning in Biomolecular Simulation. *J. Comput. Biol.* **2013**, *20*, 188−198.
(33) Oostenbrink, C.; Villa, A.; Mark, A. E.; Van Gunsteren, W. F. A Biomolecular Force Field Based on the Free Enthalpy of Hydration and Solvation: The GROMOS force-field parameter sets 53A5 and 53A6. *J. Comput. Chem.* **2004**, *25*, 1656−1676.
(34) Nosé, S. A Unified Formulation of the Constant Temperature Molecular Dynamics Methods. *J. Chem. Phys.* **1984**, *81*, 511−519.
(35) Hoover, W. G. Canonical Dynamics: Equilibrium Phase-Space Distributions. *Phys. Rev. A: At., Mol., Opt. Phys.* **1985**, *31*, 1695−1697.
(36) Frenkel, D.; Smit, B. Understanding Molecular Simulation: From Algorithms to Applications, 2nd ed.; Academic Press: San Diego, CA, 2002.
(37) Conyard, J.; Heisler, I. A.; Browne, W. R.; Feringa, B. L.; Amirjalayer, S.; Buma, W. J.; Woutersen, S.; Meech, S. R. Ultrafast Excited State Dynamics in 9,9′-Bifluorenylidene. *J. Phys. Chem. A* **2014**, *118*, 5961−5968.
(38) Pal, N.; Verma, S. D.; Sen, S. Probe Position Dependence of DNA Dynamics: Comparison of the Time-Resolved Stokes Shift of Groove-Bound to Base-Stacked Probes. *J. Am. Chem. Soc.* **2010**, *132*, 9277−9279.
(39) Sen, S.; Andreatta, D.; Ponomarev, S. Y.; Beveridge, D. L.; Berg, M. A. Dynamics of Water and Ions Near DNA: Comparison of Simulation to Time-Resolved Stokes-Shift Experiments. *J. Am. Chem. Soc.* **2009**, *131*, 1724−1735.
(40) Zhong, D.; Pal, S. K.; Zhang, D.; Chan, S. I.; Zewail, A. H. Femtosecond Dynamics of Rubredoxin: Tryptophan Solvation and Resonance Energy Transfer in the Protein. *Proc. Natl. Acad. Sci. U. S. A.* **2002**, *99*, 13−18.
(41) Vajda, S.; Jimenez, R.; Rosenthal, S. J.; Fidler, V.; Fleming, G. R.; Castner, E. W. Femtosecond to Nanosecond Solvation Dynamics in Pure Water and Inside the [gamma]-Cyclodextrin Cavity. *J. Chem. Soc., Faraday Trans.* **1995**, *91*, 867−873.
(42) Maroncelli, M.; Fleming, G. R. Comparison of Time-Resolved Fluorescence Stokes Shift Measurements to a Molecular Theory of Solvation Dynamics. *J. Chem. Phys.* **1988**, *89*, 875−881.
(43) Maroncelli, M.; Castner, E. W.; Bagchi, B.; Fleming, G. R. Dipolar Solvation Dynamics. *Faraday Discuss. Chem. Soc.* **1988**, *85*, 199−210.
(44) Qiu, W.; Zhang, L.; Okobiah, O.; Yang, Y.; Wang, L.; Zhong, D.; Zewail, A. H. Ultrafast Solvation Dynamics of Human Serum Albumin: Correlations with Conformational Transitions and Site-Selected Recognition. *J. Phys. Chem. B* **2006**, *110*, 10540−10549.
(45) Pal, S. K.; Peon, J.; Zewail, A. H. Biological Water at the Protein Surface: Dynamical Solvation Probed Directly with Femtosecond Resolution. *Proc. Natl. Acad. Sci. U. S. A.* **2002**, *99*, 1763−1768.
(46) Zewail, A. H. Femtochemistry: The Role of Alignment and Orientation. *J. Chem. Soc., Faraday Trans. 2* **1989**, *85*, 1221−1242.
(47) Reynolds, L.; Gardecki, J. A.; Frankland, S. J. V.; Horng, M. L.; Maroncelli, M. Dipole Solvation in Nondipolar Solvents: Experimental Studies of Reorganization Energies and Solvation Dynamics†. *J. Phys. Chem.* **1996**, *100*, 10337−10354.
(48) Rosenthal, S. J.; Jimenez, R.; Fleming, G. R.; Kumar, P. V.; Maroncelli, M. Solvation Dynamics in Methanol: Experimental and Molecular Dynamics Simulation Studies. *J. Mol. Liq.* **1994**, *60*, 25−56.
(49) Maroncelli, M.; Kumar, P. V.; Papazyan, A.; Horng, M. L.; Rosenthal, S. J.; Fleming, G. R. Studies of the Inertial Component of Polar Solvation Dynamics. *AIP Conf. Proc.* **1993**, *298*, 310−333.
(50) Rosenthal, S. J.; Xie, X.; Du, M.; Fleming, G. R. Femtosecond Solvation Dynamics in Acetonitrile: Observation of the Inertial Contribution to the Solvent Response. *J. Chem. Phys.* **1991**, *95*, 4715−4718.

DOI: 10.1021/acs.jpcb.7b03420
J. Phys. Chem. B 2017, 121, 7681−7688